Quantum calculations of ^{238}U+^{238}U collision dynamics

Cédric Golabek
GANIL (IN2P3/CNRS - DSM/CEA), BP 55027, F-14076 Caen Cedex 5, France.

Cédric Simenel
CEA, Centre de Saclay, IRFU/Service de Physique Nucléaire, F-91191 Gif-sur-Yvette, France.
(Dated: February 13, 2009)

Collisions of actinide nuclei form, during very short times of few 10^{-21} s, the heaviest ensembles of interacting nucleons available on Earth. In addition to provide an excellent probe to test nuclear many-body models, such very heavy ions collisions have been proposed as an alternative way to produce heavy and superheavy elements in one hand, and to study the physics of super-strong electric fields in the other hand. If quantum electrodynamics (QED) is true, and if the life time of the giant system is of the order of few 10^{-21} s, this electric field should induce spontaneous electron-positron pair emissions from vacuum. We use the time-dependent Hartree-Fock theory which is a fully microscopic quantum approach to study collision dynamics of two ^{238}U atomic nuclei. In particular, we emphasize the role of nuclear deformation on collision time and on reaction mechanisms such as nucleon transfer or formation of three fragments. Though these calculations are pessimistic in terms of transfermium elements ($Z > 100$) production in their ground state, hot (fissioning) superheavy systems up to 130 protons might be produced at high center of mass energy (above 1300 MeV). In addition, highest collision times ($\sim 4 \times 10^{-21}$ s at 1200 MeV) should fit the necessary condition for noticeable change in the positron spectra due to static electron-positron pair creation.

The study of collisions between very heavy atomic nuclei started in the late 70s with the availability of actinide beams with sufficient energy to overcome the so-called Coulomb barrier between reactants. Collisions of two Uranium or heavier nuclei were then used to investigate two important scientific fields : the quest for super-heavy elements (SHE) [1] and the physics of super-strong electric fields [2]. In one hand, SHEs are searched to localize the next island of stability in the top of the nuclear chart [3–10] which should impact the next generation of quantum models attacking the nuclear many body problem as the existence of SHEs relies only on quantum shell effects. Indeed, in a purely classical world, i.e., without shell structure, transfermium nuclei ($Z > 100$) would undergo fission within about 10^{-20} s due to the strong repulsion between their protons.In the other hand, SHEs provide a crucial test to modern atomic models as their chemical properties might deviate from their homologue elements in the periodic table due to strong relativistic effects on the valence electron shells [11–14]. Recently, SHEs have been synthesized with "cold" fusion reactions based on closed shell target nuclei [4, 8] and with "hot" fusion reactions involving actinide targets [3, 7, 9] where nuclei up to $Z = 118$ have been produced. However, the decay chains of nuclei formed by hot fusion do not populate presently known nuclei and a "blank spot" exists in the nuclear chart around $Z = 105$ and $N = 160$. Modern experimental technics might be used to explore this region with multinucleon transfer between heavy actinides [15]. Theoretical investigations of very heavy nuclei collision dynamics are then strongly encouraged by experimentalists of the SHE community.

Very heavy ions collisions have also been used to produce super-strong electric fields. Indeed, a giant system with total charge $Z \geq 173$ may induce spontaneous electron-positron pair emissions from vacuum by a fundamental quantum electrodynamics (QED) process [16, 17]. However, no experimental evidence of this process has been obtained so far [18]. Once again, the keypoint might be a good understanding of collision dynamics, in particular collision time. In the ^{238}U+^{238}U reaction, say, the static e^+e^- pair creation is expected to modify noticeably the positron spectra for sticking times of several 10^{-21} s as shown by recent theoretical calculations based on the time-dependent Dirac equation [19].

A naive estimation involving Rutherford trajectory leads to very short times ($\sim 10^{-21}$ s) during which the nuclei overlap. Though no pocket exists in the nucleus-nucleus potential of, say, the ^{238}U+^{238}U system [20], nuclear attraction reduces Coulomb repulsion in one hand and other dissipation mechanisms as evolution of nuclear shapes may delay the separation of the system in the other hand [15]. Experimentally, collision times have been estimated from oscillations in $\delta-$electron spectra [21] and values of $\sim 2 \times 10^{-21}$ s have been obtained in ^{238}U+^{238}U above the barrier [22]. On the theoretical side, macroscopic models have first been used (see, e.g., ref. [15]). However, the complexity of reaction mechanisms and the high number of degrees of freedom to be included in realistic calculations motivate the use of microscopic approaches. First microscopic calculations of the collision of two ^{238}U nuclei have been performed recently thanks to the Quantum Molecular Dynamics (QMD) model [23]. Though a major step forward has been done in terms of predictive power with these calculations, improvement are mandatory for a more real-

istic description of collision dynamics. For instance, the strong static deformation of ^{238}U ground state is not included and nucleon wave functions are constrained to be Gaussian wave packets. In addition, the Pauli principle is only approximately treated in QMD.

In this work, we present the first fully microscopic quantum calculation of the ^{238}U+^{238}U collision dynamics without any constraint on the form of the nucleon wave functions. In addition to quantitative predictions of collision times, we investigate the problem of how orientation of deformed collision partners affects dynamics.

We use the time dependent Hartree-Fock (TDHF) theory proposed by Dirac [24] with a Skyrme energy density functional (EDF) modeling nuclear interactions between nucleons [25]. The EDF is the only phenomenological ingredient of the model, as it has been adjusted on nuclear structure properties like infinite nuclear matter and radii and masses of few doubly magic nuclei [26]. The main approximation of the theory is to constrain the many-body wave function to be an antisymetrized independent particles state at any time. The latter ensures an exact treatment of the Pauli principle during time evolution. Though TDHF does not include two-body collision term, it is expected to treat correctly one-body dissipation which is known to drive low energy reaction mechanisms as Pauli blocking prevents nucleon-nucleon collisions. At initial time, the nuclei are in their Hartree-Fock ground state allowing for a fully consistent treatment of nuclear structure and dynamics.

The TDHF equation can be written as a Liouville-Von Neumann equation

$$i\hbar\frac{\partial}{\partial t}\rho = [h[\rho], \rho] \tag{1}$$

where ρ is the one body density matrix associated to the total independent particles state with elements

$$\rho(\mathbf{r}sq, \mathbf{r}'s'q') = \sum_{i=1}^{A_1+A_2} \varphi_i(\mathbf{r}sq)\varphi_i^*(\mathbf{r}'s'q'). \tag{2}$$

The sum runs over all occupied single particle wave functions φ_i and $\mathbf{r}$, s and q denote the position, spin and isospin of the nucleon respectively. The Hartree-Fock single particle Hamiltonian $h[\rho]$ is related to the EDF, noted $E[\rho]$, by its first derivative

$$h[\rho](\mathbf{r}sq, \mathbf{r}'s'q') = \frac{\delta E[\rho]}{\delta\rho(\mathbf{r}'s'q', \mathbf{r}sq)}. \tag{3}$$

First applications of TDHF to nuclear collisions were restricted to calculations in one dimension [27]. Recent increase of computational power allowed realistic TDHF calculations of heavy ions collisions in 3 dimensions with modern Skyrme functionals including spin-orbit term [28, 29]. In this work, Eq. 1 is solved iteratively in time on a spatial grid with a plane of symmetry (the collision plane) using the TDHF3D code built by P. Bonche and coworkers with the SLy4d parameterization of the Skyrme EDF [28]. The step size of the network is 0.8 fm and the step time 1.5×10^{-24} s. This code has been extensively used to study heavy ions fusion [30–34]. In particular, it reproduces average fusion barriers very well without any additional parameter than the EDF ones, i.e., with no input from reaction mechanisms [33, 34].

The ^{238}U nucleus exhibits a prolate deformation in its ground state. Its deformation axis is also a symmetry axis. In order to investigate the role of this deformation on collision dynamics, we present results on four configurations associated to different initial orientations. In the xx (respectively yy) configuration, both deformation axis are parallel to each other and parallel (resp. perpendicular) to the collision axis x. In the yx configuration, one nucleus is aligned and one is perpendicular to the collision axis, while in the yz one, both deformation axis are perpendicular to the collision axis in addition to be perpendicular to each other. We present results on central collisions only as they lead to the most dissipative reactions with the longest collision times.

The importance of initial orientation on reaction mechanism is clearly seen in Figure 1. Snapshots of isodensities at half saturation density, i.e., $\rho_0/2 = 0.08$ fm^{-3}, are plotted for the xx, yx and yy configurations at a center of mass energy $E_{CM} = 900$ MeV. We observe very different behaviors, e.g., the xx configuration is the only one which produces three fragments in the exit channel. The yy configuration gives two symmetric fragments due to an $x = 0$ plane of symmetry. Though nucleon transfer is still possible in the yy configuration thanks to fluctuations, it is expected to be stronger in the yx configuration because, in addition to fluctuations, no spatial symmetry prevents from an average flux of nucleons from one nucleus to the other. Indeed, integration of proton and neutron densities in each side of the box after the yx collision indicates an average transfer of ~ 6 protons and ~ 11 neutrons from the right to the left. In this case, transfer occurs from the tip of the aligned nucleus to the side of the other.

To get a deeper insight into the transfer in the yx configuration, we investigate the role of collision energy. The latter is plotted in Figure 2-a. Two regimes can clearly be identified. At $E_{CM} \leq 1000$ MeV, usual transfer occurs, i.e., single particle wave functions are transfered through the neck with a smooth change of the shapes of the fragments. In particular, the particle density in the neck increases with energy but is always lower than the saturation density $\rho_0 = 0.16$ fm^{-3}. The latter value is reached only at $E_{CM} \sim 1000$ MeV. At higher energies, however, the contact area gets more dense and a close look at densities along the collision axis indicates dynamical fluctuations with increasing amplitudes when energy increases. The propagation of these fluctuations of internal density modifies the breaking point of the gi-

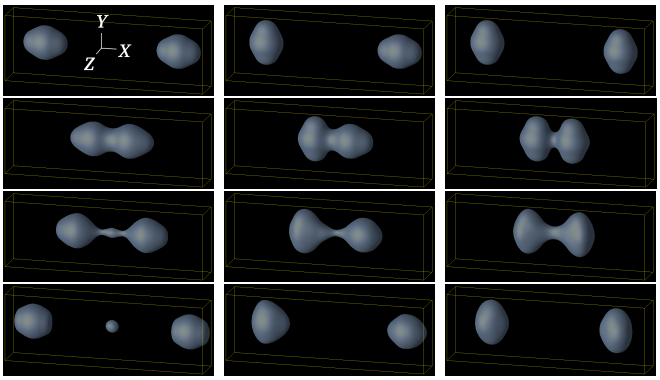

FIG. 1: Isodensities at half the saturation density in ^{238}U+^{238}U central collision at a center of mass energy E_{CM} = 900 MeV. Evolutions associated to the three initial configurations xx, yx and yy are plotted in the left, middle and right column respectively. Snapshots are given at times t = 0, 15, 27 and 42 $\times 10^{-22}$ s from top to bottom.

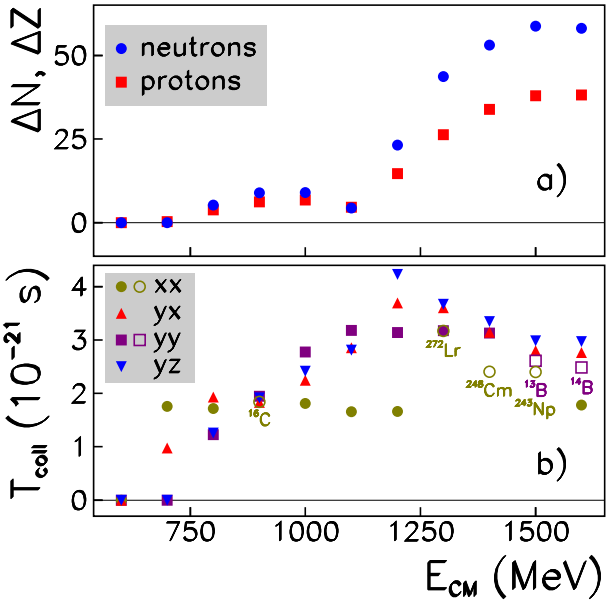

FIG. 2: a) Number of transfered nucleons in the yx configuration and b) collision times for each orientation as function of center of mass energy. Empty symbols indicate that three fragments are produced in the exit channel. In this case, the closest nucleus to the middle fragment is given.

ant system in such a way that the left fragment gains much more nucleons than expected in usual transfer. At energies above 1600 MeV (not shown on Fig. 2), density fluctuations are such that transfer in the opposite direction occurs too (from the left fragment to the right). Superheavy fragments up to $Z \sim 130$ and $N \sim 205$ could be produced at $\sim$ 1500 MeV. However, such a violent collision is expected to leave the heavy fragment with very high temperature in such a way that it decays spontaneously into statistical fission. At lower energy, in particular in the usual transfer regime ($E_{CM} \leq 1000$ MeV), the heavy fragment may survive to fission but is not expected to reach the SHE island of stability. Indeed, the heaviest fragment in this energy range is ^{253}Cf in our calculations. Note that this is consistent with experiment as no transfermium nuclei ($Z > 100$) have been observed in this reaction and energy range [1].

As can be seen in the xx case in Figure 1, the system may also produce a small fragment in the center of the box, a feature which is similar to what have been observed ten years ago in spontaneous ternary fission of ^{252}Cf [35]. Here, integration of proton and neutron densities indicates a ^{16}C-like fragment. Why the system decides to form a third fragment instead of breaking at the neck? Again, the answer is given by a close look at the internal density of the system. Figure 3 shows a snapshot of the density in the collision plane obtained in the xx configuration at E_{CM} = 900 MeV at closest approach. We see a strong overlap of the fragment tips and the density reaches a maximum of 0.166 fm^{-3} in the neck, exceeding saturation density ρ_0. Thus, the system breaks on both sides of this density excess and forms a small fragment in the middle. At higher energies, however, the excess of density is higher and propagates rapidly in the giant system. The latter then breaks either in two Uranium-like fragments, or in three fragments with a heavy one in the middle (see Figure 2-b). Note that for such violent collisions, the collision term which is negligible at low energy might play a role. Extensions of TDHF including collision term should then be considered to check these predictions when densities well above saturation density are reached. Finally, three fragments are also obtained in the exit channel of the yy configuration at E_{CM} = 1500 and 1600 MeV. Here, the middle fragment corresponds to a neutron rich Boron isotope (see Figure 2-b). It occurs at higher energy than in the xx case because a closest distance is needed to overcome the saturation density in the neck. The latter is reached at $\sim$ 1200 MeV in the yy configuration. Note that overcoming saturation density is not a sufficient condition to produce three fragments as, e.g., we do not observe such an exit channel in the yz configuration.

Let us finally investigate a last important aspect of collision dynamics, namely the collision time between nuclei. We define the latter as the time during which the neck density exceeds $\rho_0/10$ = 0.016 fm^{-3}. Figure 2-b shows the evolution of collision time T_{coll} as a function of E_{CM} for each configuration. In the low energy part ($E_{CM} \leq 900$ MeV), we clearly see three distinct behaviors between the xx, yx and yy/yz configurations. For instance, the latter need more energy to get into contact as the energy threshold above which nuclear interaction plays a significant role is higher for compact configurations.

Looking now at the all energy range, we see that the yx, yy and yz orientations exhibit roughly the same be-

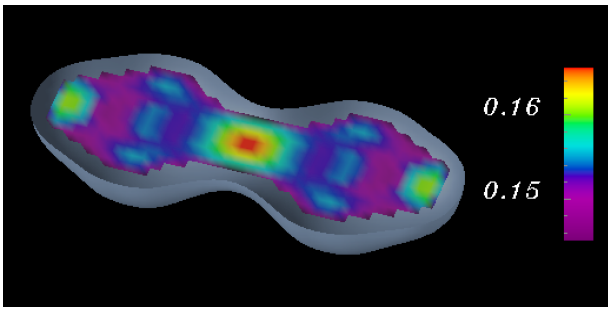

FIG. 3: Nucleon density in fm^{-3} in the collision plane at closest approach ($t = 1.36 \times 10^{-21}$ s) in the xx configuration at $E_{CM} = 900$ MeV.

havior, i.e., a rise and fall of T_{coll} with a maximum of $3 - 4 \times 10^{-21}$ s at $E_{CM} \sim 1200$ MeV, in agreement with the QMD calculations of ref. [23]. Dynamical evolution of nuclear shapes in these three configurations, in addition to a strong transfer in the yx one (see Figure 2-a) are responsible for these rather long collision times as compared to scattering with frozen shapes of the reactants [15]. The xx configuration, however, behaves differently. In this case, T_{coll} exhibits a plateau which does not exceed 2×10^{-21} s except when three fragments are formed in the exit channel with a heavy one in the center for which longer collision times are obtained due to dynamical density fluctuations. This overall reduction of T_{coll} in the xx case is attributed to the strong overlap of the tips. Indeed, as we already see at $E_{CM} = 900$ MeV in Figure 3, this overlap produces a density in the neck much higher than saturation density. The fact that nuclear matter is difficult to compress translates into a strong repulsive force between the fragments which decreases their contact time. This phenomenon is also responsible for the fall of collision times in the other configurations, though occurring at higher energies due to the fact that closer distances between the reactants are needed to strongly overlap.

To conclude, this first fully microscopic quantum investigation of collision dynamics of two Uranium nuclei exhibits a rich phenomenology which is strongly influenced by the shape of the atomic nuclei. Depending on their orientations, two or three fragments are produced in the exit channel. The average number of transfered nucleons is also strongly affected. At high energy, dynamical effects are expected to enhance this transfer producing hot primary fragments up to $Z \sim 130$ protons in average. Heavy fragments produced at low energy might survive fission, but the center of their charge distribution is not expected to reach the transfermium region. This indicates that this reaction might not be apropriate to populate the blank spot region of the nuclear chart beween decay chains of superheavy elements produced by "hot" and "cold" fusion. Other reactions as ^{238}U+^{248}Cm might be more efficient [15]. Finally, our calculations show that the giant system might survive enough time (up to 4×10^{-21}s at an energy of 1200 MeV in the center of mass) to test nonperturbative QED with super-strong electric fields.

We thank P. Bonche for providing his code. The calculations have been performed in the Centre de Calcul Recherche et Technologie of the Commissariat à l'Énergie Atomique.

[1] M. Schädel *et al.*, Phys. Rev. Lett. **41**, 469 (1978).
[2] J. Schweppe *et al.*, Phys. Rev. Lett. **51**, 2261 (1983).
[3] Yu. Ts. Oganessian *et al.*, Nature **400**, 242 (1999).
[4] S. Hofmann and G. Münzenberg, Rev. Mod. Phys. **72**, 733 (2000).
[5] S. Ćwiok, P.-H. Heenen, and W. Nazarewicz, Nature **433**, 705 (2005).
[6] R.-D. Herzberg *et al.*, Nature **442**, 896 (2006).
[7] Yu. Ts. Oganessian *et al.*, Phys. Rev. C **74**, 044602 (2006).
[8] K. Morita *et al.*, J. Phys. Soc. Jpn. **76**, 045001 (2007).
[9] S. Hofmann *et al.*, Eur. Phys. J. A **32**, 251 (2007).
[10] M. Morjean *et al.*, Phys. Rev. Lett. **101**, 072701 (2008).
[11] M. Schdel *et al.*, Nature **388**, 55 (1997).
[12] R. Eichler *et al.*, Nature **407**, 63 (2000).
[13] Ch. E. Düllmann *et al.*, Nature **418**, 859 (2002).
[14] R. Eichler *et al.*, Nature **447**, 72 (2007).
[15] V. I. Zagrebaev, Yu. Ts. Oganessian, M. G. Itkis, and W. Greiner, Phys. Rev. C **73**, 031602(R) (2006).
[16] J. Reinhardt, B. Müller, and W. Greiner, Phys. Rev. A **24**, 103 (1981).
[17] *Quantum Electrodynamics of Strong Fields*, edited by W. Greiner (Plenum, New York, 1983).
[18] I. Ahmad *et al.*, Phys. Rev. C **60**, 064601 (1999).
[19] E. Ackad and M. Horbatsch, Phys. Rev. A **78**, 062711 (2008).
[20] J. F. Berger, J. D. Anderson, P. Bonche, and M. S. Weiss, Phys. Rev. C **41**, 6 (1990).
[21] G. Soff, J. Reinhardt, B. Müller, and W. Greiner, Phys. Rev. Lett. **43**, 1981 (1979).
[22] R. Krieg *et al.*, Phys. Rev. C **34**, 562 (1986).
[23] J. Tian, X. Wu, K. Zhao, Y. Zhang, and Z. Li, Phys. Rev. C **77**, 064603 (2008).
[24] P. A. M. Dirac, Proc. Camb. Phil. Soc. **26**, 376 (1930).
[25] T. Skyrme, Phil. Mag. **1**, 1043 (1956).
[26] E. Chabanat, P. Bonche, P. Haensel, J. Meyer, and R. Schaeffer, Nucl. Phys. **A635**, 231(1998).
[27] P. Bonche, S. Koonin, and J. W. Negele, Phys. Rev. C **13**, 1226 (1976).
[28] K.-H. Kim, T. Otsuka and P. Bonche, J. Phys. G **23**, 1267 (1997).
[29] A. S. Umar and V. E. Oberacker, Phys. Rev. C **73**, 054607 (2006).
[30] C. Simenel, Ph. Chomaz and G. de France, Phys. Rev. Lett. **86**, 2971 (2001).
[31] C. Simenel, Ph. Chomaz and G. de France, Phys. Rev. Lett. **93**, 102701 (2004).
[32] C. Simenel, Ph. Chomaz and G. de France, Phys. Rev. C **76**, 024609 (2007).
[33] C. Simenel and B. Avez, Int. J. Mod. Phys. E **17**, 31

(2008).
[34] K. Washiyama and D. Lacroix, Phys. Rev. C **78**, 024610 (2008).
[35] A. V. Ramayya *et al.,* Phys. Rev. Lett. **81**, 947 (1998).